Generalized ray matrix for spherical mirror reflection and its application in square ring resonators and monolithic triaxial ring resonators

Article *in* Optics Express · March 2011

DOI: 10.1364/OE.19.006762 · Source: PubMed

3 authors, including:

Jie Yuan
National University of Defense Technology
46 PUBLICATIONS **259** CITATIONS

SEE PROFILE

Generalized ray matrix for spherical mirror reflection and its application in square ring resonators and monolithic triaxial ring resonators

Jie Yuan,* Xingwu Long and Meixiong Chen

Department of Optoelectronic Engineering, College of Opto-electric Science and Engineering, National University of Defense Technology, Hunan 410073, China
**jieyuan@nudt.edu.cn*

Abstract:To the best of our knowledge, the generalized ray matrix, an augmented 5×5 ray matrix for a spherical mirror reflection with all the possible perturbation sources including three kinds of displacements and its detailed deducing process have been proposed in this paper for the first time. Square ring resonators and monolithic triaxial ring resonators have been chosen as examples to show its application, and some novel results of the optical-axis perturbation have been obtained. A novel method to eliminate the diaphragm mismatching error and the gain capillary mismatching error in monolithic triaxial ring resonators more effectively has also been proposed. Both those results and method have been confirmed by related experiments and the experimental results have been described with diagrammatic representation. This generalized ray matrix is valuable for ray analysis of various kinds of resonators. These results are important for the cavity design, cavity improvement and alignment of high accuracy and super high accuracy ring laser gyroscopes.

OCIS codes: (140.4780) Optical resonators; (140.3410) Laser resonators; (140.3370) Laser gyroscopes; (140.3560) Lasers, ring.

References and links

1. W. W. Chow, J. Gea-Banacloche, L. M. Pedrotti, V. E. Sanders, W. Schleich, and M. O. Scully, "The ring laser gyro," Rev. Mod. Phys. **57**(1), 61–86 (1985).
2. M. Faucheux, D. Fayoux, and J. J. Roland, "The ring laser gyro," J. Opt. **19**(3), 101–115 (1988).
3. A. E. Siegman, "Laser beams and resonators: beyond the 1960s," IEEE J. Sel. Top. Quantum Electron. **6**(6), 1389–1399 (2000).
4. J. A. Arnaud, "Degenerate Optical Cavities. II: Effect of Misalignments," Appl. Opt. **8**(9), 1909–1917 (1969).
5. G. B. Altshuler, E. D. Isyanova, V. B. Karasev, A. L. Levit, V. M. Ovchinnikov, and S. F. Sharlai, "Analysis of misalignment sensitivity of ring laser resonators," Sov. J. Quantum Electron. **7**, 857–859 (1977).
6. H. R. Bilger, and G. E. Stedman, "Stability of planar ring lasers with mirror misalignment," Appl. Opt. **26**(17), 3710–3716 (1987).
7. R. Rodloff, "A laser gyro with optimized resonator geometry," IEEE J. Quantum Electron. **23**(4), 438–445 (1987).
8. J. Yuan, X. W. Long, B. Zhang, F. Wang, and H. C. Zhao, "Optical axis perturbation in folded planar ring resonators," Appl. Opt. **46**(25), 6314–6322 (2007).
9. I. W. Smith, "Optical resonator axis stability and instability from first principles," Proc. SPIE **412**, 203–206 (1983).
10. A. L. Levkit, and V. M. Ovchinnikov, "Stability of a ring resonator with a nonplane axial contour," J. Appl. Spectrosc. (USSR) **40**(6), 657–660 (1984).
11. S.-C. Sheng, "Optical-axis perturbation singularity in an out-of-plane ring resonator," Opt. Lett. **19**(10), 683–685 (1994).
12. A. H. Paxton, and W. P. Latham, Jr., "Unstable resonators with 90° beam rotation," Appl. Opt. **25**(17), 2939–2946 (1986).

#141768 - $15.00 USD Received 26 Jan 2011; revised 13 Mar 2011; accepted 15 Mar 2011; published 24 Mar 2011

13. B. E. Currie, G. E. Stedman, and R. W. Dunn, "Laser stability and beam steering in a nonregular polygonal cavity," Appl. Opt. **41**(9), 1689–1697 (2002).
14. J. Yuan, and X. W. Long, "Optical-axis perturbation in nonplanar ring resonators," Opt. Commun. **281**(5), 1204–1210 (2008).
15. J. Yuan, X. W. Long, and L. M. Liang, "Optical-axis perturbation in triaxial ring resonator," Appl. Opt. **47**(5), 628–631 (2008).
16. X. W. Long, and J. Yuan, "Method for eliminating mismatching error in monolithic triaxial ring resonators," Chin. Opt. Lett. **8**(12), 1135–1138 (2010).
17. D. Z. Anderson, "Alignment of resonant optical cavities," Appl. Opt. **23**(17), 2944–2949 (1984).
18. N. M. Sampas, and D. Z. Anderson, "Stabilization of laser beam alignment to an optical resonator by heterodyne detection of off-axis modes," Appl. Opt. **29**(3), 394–403 (1990).
19. J. Yuan, and X. W. Long, "CCD-area-based autocollimator for precision small-angle measurement," Rev. Sci. Instrum. **74**(3), 1362–1365 (2003).
20. J. Yuan, X. W. Long, and K. Y. Yang, "Temperature-controlled autocollimator with ultrahigh angular measuring precision," Rev. Sci. Instrum. **76**(12), 125106 (2005).

1. Introduction

There have been some kinds of planar or nonplanar, monoaxial or monolithic triaxial ring resonators (MTRR), which are widely used for laser gyroscopes [1–3]. Ray matrix method have been widely used for analyzing the optical-axis perturbation in planar or nonplanar ring resonators [4–14]. Nonplanar ring resonators have modified misalignment or optical-axis stability properties as analyzed by several authors [9–14]. Optical-axis perturbation of MTRR have also been discussed in our previous articles [15, 16]. However, the perturbation sources in most of the previous articles are angular misalignments of the optical components of the ring resonator. For a spherical mirror, the perturbation source of the radial displacements have not been discussed before, and the perturbation source of the axial displacement has not been discussed in detail before [15, 16]. The detailed coordinate system for deducing the ray matrix have not been analyzed in previous papers too.

The augmented 5×5 ray matrix method is widely used for handling those perturbation sources, and it has been explained in previous articles [8, 11, 14–16]. In this paper, the generalized ray matrix, an augmented 5×5 ray matrix for a mirror which includes the perturbation sources of both the mirror's angular misalignments and the mirror's displacements has been proposed for the first time. The detailed coordinate system for deducing the ray matrix has been proposed too. To the best of our knowledge, this is the first time the perturbations due to mirror axial displacement and radial displacements are accurately considered. The square ring resonator (SRR) and MTRR will be chosen as examples to show its application. Based on the augmented 5×5 ray matrix method by considering four mirror's axial displacement and two spherical mirror's radial displacements in SRR and MTRR, the rules of the optical-axis perturbation have been obtained. The relationship between the diaphragm mismatching error C of the MTRR, which has been proposed in our previous paper [15], and the entire four mirror's axial displacement has been found out. In this paper, the gain capillary mismatching error $C2$ of the MTRR has been defined, and a novel method to eliminate the mismatching errors C and $C2$ more effectively has been proposed. By utilizing this method, the mismatching errors C and $C2$ can be reduced to 0 simultaneously. Both the rules of the optical-axis perturbation and the eliminating method will be described in detail with diagrammatic representation.

2. Analysis method

The ray matrix of a general optical component with angular misalignment and translational displacements has the form

#141768 - $15.00 USD Received 26 Jan 2011; revised 13 Mar 2011; accepted 15 Mar 2011; published 24 Mar 2011

$$\begin{pmatrix} r_{ox} \\ r_{ox}^{'} \\ r_{oy} \\ r_{oy}^{'} \\ 1 \end{pmatrix} = \begin{pmatrix} A_x & B_x & 0 & 0 & E_x \\ C_x & D_x & 0 & 0 & F_x \\ 0 & 0 & A_y & B_y & E_y \\ 0 & 0 & C_y & D_y & F_y \\ 0 & 0 & 0 & 0 & 1 \end{pmatrix} \begin{pmatrix} r_{ix} \\ r_{ix}^{'} \\ r_{iy} \\ r_{iy}^{'} \\ 1 \end{pmatrix}, \tag{1}$$

where r_{ix}, r_{iy}, r_{ox} and r_{oy} are the input ray and output ray heights from the reference axis along the x and y axes respectively and we call them optical-axis decentration. $r_{ix}^{'}$, $r_{iy}^{'}$, $r_{ox}^{'}$ and $r_{oy}^{'}$ are the angles that the input ray and output ray makes with the reference axis in the x and y plane respectively and we call them optical-axis tilt. A_x, B_x, C_x and D_x are the standard ray-matrix elements in tangential plane, A_y, B_y, C_y and D_y are the standard ray-matrix elements in sagittal plane, E_x and E_y are the decentration terms which represent radial displacements along x and y axes. F_x and F_y are the tilt terms which represent the angular misalignments.

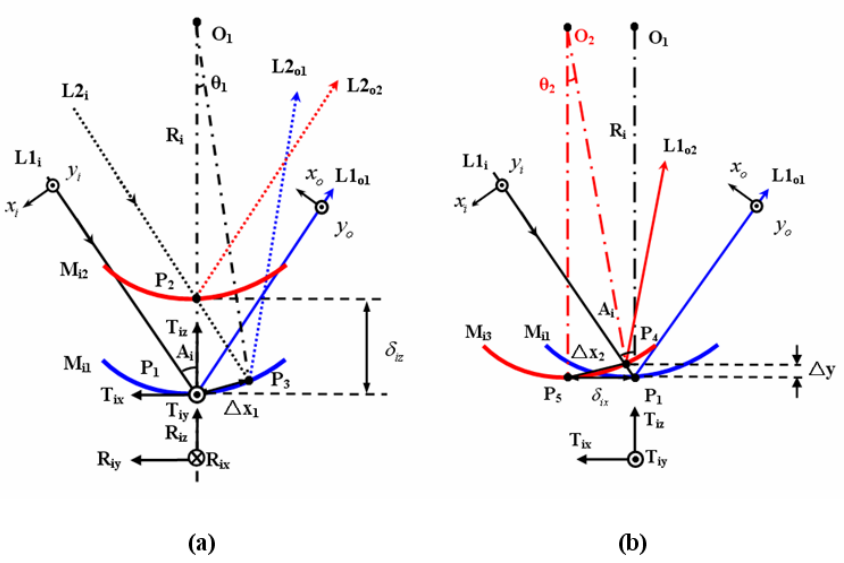

Fig. 1. Translational displacements of a spherical mirror M_i. (a) axial displacement δ_{iz} of M_i and (b) radial displacement δ_{ix} of M_i. R_i: the radius of spherical mirror M_i, A_i: the incident angle, M_{i1}: the blue solid arc which is the initial position of M_i, M_{i2}: the red solid arc in (a) which is the position of M_i after axial displacement δ_{iz}, M_{i3}: the red solid arc in (b) which is the position of M_i after radial displacement δ_{ix}, P_1, P_2, P_3, P_4 and P_5: the reflecting points, O_1 and O_2: spherical centers of M_{i1} and M_{i3}, T_{ix}, T_{iy} and T_{iz}: three translational axes, R_{ix}, R_{iy} and R_{iz}: three rotational axes, L_{1i} and L_{2i}: two parallel incident rays, L_{1o1}, L_{1o2}, L_{2o1} and L_{2o2}: four reflection rays, x_i and y_i: the coordinate axes of the incident ray, x_o and y_o: the coordinate axes of the reflected ray, θ_1: the angle between line O_1P_1 and line O_1P_3, θ_2: the angle between line O_2P_4 and line O_2P_5, Δx_1: the distance between P_1 and P_3, Δx_2: the distance between P_4 and P_5, Δy: the distance between P_1 and P_4.

#141768 - $15.00 USD Received 26 Jan 2011; revised 13 Mar 2011; accepted 15 Mar 2011; published 24 Mar 2011

A spherical mirror M_i with radius R_i has been chosen as an example to show the perturbation sources in Fig. 1 and Fig. 2. The incident angle is A_i. As shown in Fig. 1(a), generally the mirror M_i has 3 kinds of translational displacements and 3 kinds of angular misalignments. δ_{ix}, δ_{iy} and δ_{iz} are three kinds of translational displacements along the axes of T_{ix}, T_{iy} and T_{iz} respectively. θ_{ix}, θ_{iy} and θ_{iz} are three kind of angular misalignments around the axes of R_{ix}, R_{iy} and R_{iz} respectively. θ_{iz} can be ignored because the mirror has a spherical symmetry.

In summary, θ_{ix}, θ_{iy}, δ_{ix}, δ_{iy}, and δ_{iz} are 5 kinds of possible perturbation sources for a spherical mirror. θ_{ix} and θ_{iy} are angular misalignments. In this paper, δ_{ix} and δ_{iy} are called radial displacements, and δ_{iz} is called axial displacement.

The axial displacement has not been discussed in detail before. The 5×5 ray matrix for a mirror which has been proposed in our previous paper is not applicable [16]. To the best of our knowledge, this is the first time a generalized 5×5 ray matrix for a mirror with all of the 5 possible perturbation sources is proposed and detailed coordinate system for deriving this matrix is presented.

The axial displacement δ_{iz} will be analyzed first. As shown in Fig. 1(a), M_{i1} and M_{i2} represent the mirror M_i before and after the axial displacement δ_{iz}. The reflection point has been changed from point P_1 and to point P_2. For a linear resonator, the ray is incident vertically and $A_i = 0$. The transversal offset between P_1 and P_2 is zero and the reflection point has not been changed under the axial displacement δ_{iz}. For a ring resonator, the ray is not incident vertically and $A_i \neq 0$. To discuss this effect in detail, two parallel incident rays $L1_i$ and $L2_i$ are chosen for examples. $L1_{o1}$ is the reflection ray of $L1_i$ via the reflection at the point P_1 of M_{i1}. $L2_{o1}$ is the reflection ray of $L2_i$ via the reflection at the point P_3 of M_{i1}. $L2_{o2}$ is the reflection ray of $L2_i$ via the reflection at the point P_2 of M_{i2}. The coordinate axes of the incident ray are x_i and y_i, and the coordinate axes of the reflected rays are x_o and y_o. Firstly the decentration terms which represent the radial displacement along the x and y axes are analyzed. For the incident ray $L2_i$, the coordinates of the point P_2 are $(-\delta_{iz} \times \sin(A_i), 0)$ and $(\delta_{iz} \times \sin(A_i), 0)$ in the coordinate axes of incidental ray and reflection ray respectively, so the standard ray-matrix elements $M_i(1, 5)$ should be modified into $2\delta_{iz} \times \sin(A_i)$. Secondly, the tilt terms which represent the angular misalignments are analyzed. For the reflection ray of the incident ray $L2_i$ in the coordinate axis of reflection ray, the exit angle of $L2_{o1}$ is $2\theta_1 \approx 2\Delta x_1 / R \approx 2\delta_{iz} \times \tan(A_i) / R_i$ and the exit angle of $L2_{o2}$ is 0. This angle is under the direction of x axis and the angle modification under the direction of y axis is 0, so the standard ray-matrix elements $M_i(2, 5)$ should be modified into $-2\delta_{iz} \times \tan(A_i) / R_i$. The case which is shown in Fig. 1 is that the angle between the positive directions of x_i and δ_{iz} is bigger than 90 degree. If the angle is smaller than 90 degree, the standard ray-matrix elements $M_i(1, 5)$ and $M_i(2, 5)$ should be modified into $-2\delta_{iz} \times \sin(A_i)$ and $2\delta_{iz} \times \tan(A_i) / R_i$ respectively.

The spherical mirror's radial displacements δ_{ix} and δ_{iy} need to be considered too. As shown in Fig. 1(b), radial displacement δ_{ix} has been chosen as example for analysis. Firstly the decentration terms which represent the radial displacement along the x and y axes are analyzed. For the incident ray $L1_i$, the coordinates of the point P_4 are $(0, 0)$ and $(\Delta y \times \sin(A_i), 0)$ in the coordinate axes of incidental ray and reflection ray respectively, so

#141768 - $15.00 USD Received 26 Jan 2011; revised 13 Mar 2011; accepted 15 Mar 2011; published 24 Mar 2011

the standard ray-matrix elements $M_i(1, 5)$ should be modified into $2\Delta y \times \sin(A_i) \approx \frac{2\delta_{ix}^{\ 2}}{R_i} \times \sin(A_i)$. This term can be ignored in this paper because $\delta_{ix} << R_i$. The exit angle of $L1_{o2}$ is $2\theta_2 \approx 2\Delta x_2 / R_i \approx 2\delta_{ix} \times \tan(A_i) / R_i$ and the exit angle of $L1_{o1}$ is 0. This angle is under the direction of x axis and the angle modification under the direction of y axis is 0, so the standard ray-matrix elements $M_i(2, 5)$ should be modified into $2\delta_{ix} \times \tan(A_i) / R_i$. Similarly, the standard ray-matrix elements $M_i(4, 5)$ should be modified into $2\delta_{iy} \times \tan(A_i) / R_i$ with the consideration of spherical mirror's radial displacement δ_{iy}.

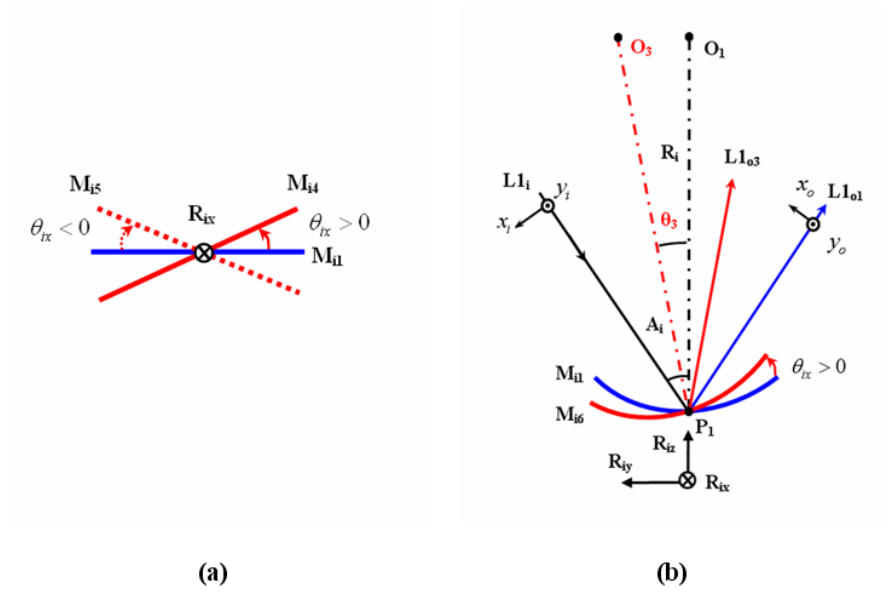

Fig. 2. Angular misalignments of a spherical mirror M_i. (a) definition of a mirror's misalignments angle θ_{ix} and (b) angular misalignment of the spherical mirror M_i around rotational axis R_{ix}. R_i: the radius of spherical mirror M_i, A_i: the incident angle, M_{i4}: the red solid line which is the position of M_i after angular misalignment $\theta_{ix} > 0$, M_{i5}: the red dashed line which is the position of M_i after angular misalignment $\theta_{ix} < 0$, M_{i1}: the blue solid arc which is the initial position of M_i, M_{i6}: the red solid arc which is the position of M_i after angular misalignment $\theta_{ix} < 0$, P_1: the reflecting points, O_1 and O_3: spherical centers of M_{i1} and M_{i6}, R_{ix}, R_{iy} and R_{iz}: three rotational axes, L_{1i}: incident ray, L_{1o1} and L_{1o3}: two reflection rays, x_i and y_i: the coordinate axes of the incident ray, x_o and y_o: the coordinate axes of the reflected ray. θ_3: the angle between P_1O_1 and P_1O_3.

As shown in Fig. 2(a), the angular misalignment θ_{ix} has been chosen as example to show the definitions of θ_{ix}, θ_{iy} and θ_{iz}. We look at the mirror M_i behind the rotation axis R_{ix}. When the mirror rotates clockwise with respect to its rotation axis R_{ix}, the induced misalignment angle of θ_{ix} is negative and $\theta_{ix} < 0$. When the mirror rotates counterclockwise with respect to its rotation axis R_{ix}, the induced misalignment angle of θ_{ix}

#141768 - $15.00 USD Received 26 Jan 2011; revised 13 Mar 2011; accepted 15 Mar 2011; published 24 Mar 2011

is positive and $\theta_{ix} > 0$. The misalignment angles of θ_{iy} and θ_{iz} are defined similarly. θ_{iz} can be ignored because the mirror has a spherical symmetry.

The angular misalignment θ_{ix} has been chosen as example for analysis in Fig. 2(b). Firstly the decentration terms which represent the radial displacement along the x and y axes are analyzed. For the incident ray $L1_i$, the coordinates of the point P_1 are both $(0,0)$ in the coordinate axes of incidental ray and reflection ray, so the standard ray-matrix elements $M_i(1, 5)$ should not be modified. The exit angle of $L1_{o3}$ is $2\theta_3 = 2\theta_{ix}$ and the exit angle of $L1_{o1}$ is 0. This angle is under the direction of x axis and the angle modification under the direction of y axis is 0, so the standard ray-matrix elements $M_i(2, 5)$ should be modified into $2\theta_{ix}$. Similarly, the standard ray-matrix elements $M_i(4, 5)$ should be modified into $2\theta_{iy}$ with the consideration of mirror's angular misalignment θ_{iy}.

In summary, a generalized ray matrix for a mirror M_i with all kinds of possible perturbation sources including δ_{ix}, δ_{iy}, δ_{iz}, θ_{ix}, and θ_{iy} (θ_{iz} can be ignored) can be written as:

$$M(M_i) = \begin{bmatrix} 1 & 0 & 0 & 0 & 2\delta_{iz} \cdot \sin(A_i) \\ -\dfrac{2}{R_i \times \cos(A_i)} & 1 & 0 & 0 & -2\delta_{iz} \cdot \tan(A_i)/R_i + 2(\theta_{ix} + \delta_{ix}/R_i) \\ 0 & 0 & 1 & 0 & 0 \\ 0 & 0 & -\dfrac{2 \times \cos(A_i)}{R_i} & 1 & 2(\theta_{iy} + \delta_{iy}/R_i) \\ 0 & 0 & 0 & 0 & 1 \end{bmatrix} \quad (2)$$

3. Analysis of square ring resonators

SRR has been chosen as an example in this paper. As shown in Fig. 3(a), the optical-axis locations x_e, y_e, x_g and y_g are the optical-axis deviations from the longitudinal axis of the ideal diaphragm and the center of the longest gain capillary along the x and y axes respectively, and the center of the longest gain capillary is also the center of the gain medium. The positive orientation of x_e, y_e, x_g and y_g are shown in Fig. 3(a). For a high accuracy laser gyro, in order to make the total diffraction loss be lowest and to improve the performance, it would be much better to make the optical-axis pass through the center of the diaphragm (point e) and the center of the gain capillary (point g) simultaneously.

Planar mirror's radial displacements $\delta_{ix}, \delta_{iy} (i = c, d)$ can be ignored because planar mirrors $M_i (i = c, d)$ have a radius of ∞. For a ring laser cavity after machining, the angles of the terminal surfaces have been determined. This means that the angular misalignments $\theta_{ix}, \theta_{iy} (i = a, b, c, d)$ caused by the angles of the terminal surfaces are 0. In summary, the simplified perturbation sources of $\delta_{iz} (i = a, b, c, d)$ and $\delta_{ix}, \delta_{iy} (i = a, b)$ should be considered and the perturbation sources of $\delta_{ix}, \delta_{iy} (i = c, d)$ and $\theta_{ix}, \theta_{iy} (i = a, b, c, d)$ should not be considered in the following discussion. The positive orientations of $\delta_{iz} (i = a, b, c, d)$ and $\delta_{ix}, \delta_{iy} (i = a, b)$ are shown in Fig. 3(a) and these orientations are their translational axes respectively. The definitions of $\delta_{iz} (i = a, b, c, d)$ and $\delta_{ix}, \delta_{iy} (i = a, b)$ are similar to the definition in Fig. 1.

#141768 - $15.00 USD Received 26 Jan 2011; revised 13 Mar 2011; accepted 15 Mar 2011; published 24 Mar 2011

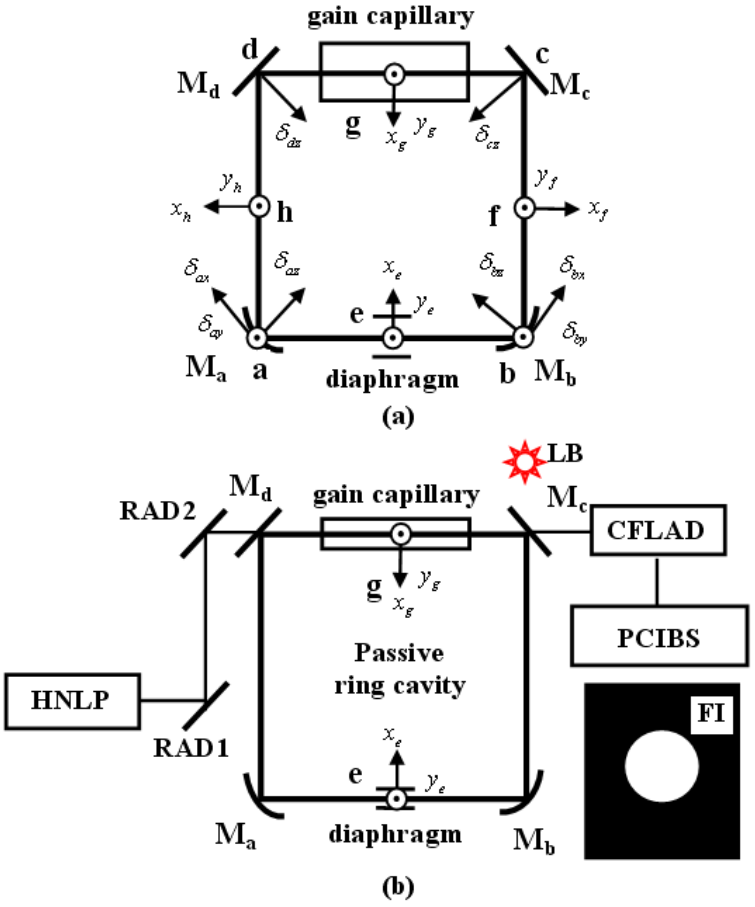

Fig. 3. (a) Schematic diagram of square ring resonator and (b) schematic diagram of alignment experiment. M_a and M_b: spherical mirrors, M_c and M_d: planar mirrors, the incident angle is 45°; a, b, c and d: terminal points of the resonator, e: the center of the diaphragm, g: the center of the gain capillary, f: the midpoint between b and c, h: the midpoint between a and d, $x_j, y_j (j = e, f, g, h)$: x and y coordinate axes at points e, f, g and h, $\delta_{iz} (i = a, b, c, d)$: axial displacement of M_i(i = a,b,c,d), $\delta_{ix}, \delta_{iy} (i = a, b)$: radial displacements of the spherical mirrors M_a and M_b, HNLP: He-Ne laser with path length control device, RAD1 and RAD2: reflectors with adjusting device, LB: light bulb, CFLAD: CCD area with focusing lens and adjusting device, PCIBS: personal computer with image grabber and image processing software, FI: facular image.

The impact of the simplified perturbation sources $\delta_{iz} (i = a, b, c, d)$ and $\delta_{ix}, \delta_{iy} (i = a, b)$ on optical-axis perturbation can be obtained by solving for the eigenvector of the total round-trip matrix of the ring resonator. Δx_e, Δy_e, Δx_g and Δy_g are the optical-axes perturbations at the center of the diaphragm (point e) and the center of the gain capillary (point g) along the x and y axes respectively, and Δx_e, Δy_e, Δx_g and Δy_g caused by the above mentioned perturbation sources can be written as

#141768 - $15.00 USD Received 26 Jan 2011; revised 13 Mar 2011; accepted 15 Mar 2011; published 24 Mar 2011

$$\Delta x_e = \frac{\sqrt{2}}{4}(\delta_{ax} + \delta_{bx} + \delta_{az} + \delta_{bz}), \Delta y_e = \frac{\sqrt{2}}{2}(\delta_{ay} + \delta_{by});$$
$$\Delta x_g = \frac{\sqrt{2}}{4}(\delta_{ax} + \delta_{bx} - \delta_{az} - \delta_{bz} + 2\delta_{cz} + 2\delta_{dz}), \Delta y_g = \frac{\sqrt{2}}{2}(\delta_{ay} + \delta_{by}). \quad (3)$$

Figure 3(b) shows schematic diagram of alignment experiment [17, 18]. The passive ring cavity is formed by two spherical mirrors (M_a and M_b) and two planar mirrors (M_c and M_d). A light bulb (LB) is used to illuminate the diaphragm and the longest gain capillary. He-Ne laser (HNLP) with wavelength $\lambda = 0.6328\mu m$ is used as laser source. The laser is reflected by two reflectors which are mounted on adjusting device (RAD1 and RAD2), and then incident into the passive ring cavity. CCD area with focusing lens which is also mounted on a adjusting device (CFLAD) is used to pick up the facular image, then the facular image (FI) is captured into the memory of a personal computer with an image grabber (PCIBS), then the image was transformed into a digital image. The center of the facular image (FI) can be obtained by image processing software (PCIBS). The image grabber has a 8 bits analog-to-digital converter, which is the light intensity range where every element of the CCD area can detect and it can be subdivided into 256 parts. The system can sense a very small deviation of the center of the facular image (FI) because the deviation causes a small alteration in the distribution of light intensity which can be sensed by the CCD area and image grabber. Special arithmetic to processing the digital image was previously published [19, 20]. The arithmetic to calculate the center of the facular image here is similar to the arithmetic to calculate the absolute position of the cross reticle image [19, 20].

First step, the light bulb (LB) is switched on and the laser (HNLP) is switched off, the facular image of illuminated diaphragm and illuminated gain capillary can be obtained respectively by adjusting the focusing lens (CFLAD). The centers of the facular image of illuminated diaphragm and illuminated gain capillary can be made both located at the center of the CCD area by adjusting the focusing lens and the adjusting device (CFLAD). The ideal optical-axis of the passive ring cavity passes through the center of the diaphragm and the center of the gain capillary. As a consequence, the optical-axis of the CCD area and focusing lens has been made aligned with the ideal optical-axis of the passive ring cavity.

Second step, spherical mirror M_a is removed from the cavity first, then the light bulb (LB) is switched off and the laser (HNLP) is switched on. The facular image of incidental laser at different locations can be obtained by adjusting the focusing lens (CFLAD). The centers of the facular image of the incidental laser at different locations can be made located at the center of the CCD area by adjusting the focusing lens and the adjusting device of two reflectors (RAD1 and RAD2). As a consequence, the optical-axis of the incidental laser has been made aligned with the optical-axis of the CCD area and focusing lens and the ideal optical-axis of the passive ring cavity too.

Third step, spherical mirror M_a is mounted on the cavity first, then the path length control device of laser (HNLP) is adjusted and the frequency of the input laser is modified, when the input frequency has a resonance with the passive ring cavity, the centers of the beam frequency facular images at point e and g can be obtained by adjusting the focusing lens (CFLAD). The optical-axis of the beam transmitted by the resonator is called the real optical-axis in this paper and it passes through the centers of the beam frequency facular images at point e and g. When the perturbation sources of $\delta_{iz}(i = a, b, c, d)$ and $\delta_{ix}, \delta_{iy}(i = a, b)$ is added to the mirrors of passive ring cavity, the real optical axis will modified with respect to the ideal optical-axis of the passive ring cavity accordingly. As a consequence, the rules of optical-axis perturbation have been obtained and the results in Eq. (3) have been confirmed.

#141768 - $15.00 USD Received 26 Jan 2011; revised 13 Mar 2011; accepted 15 Mar 2011; published 24 Mar 2011

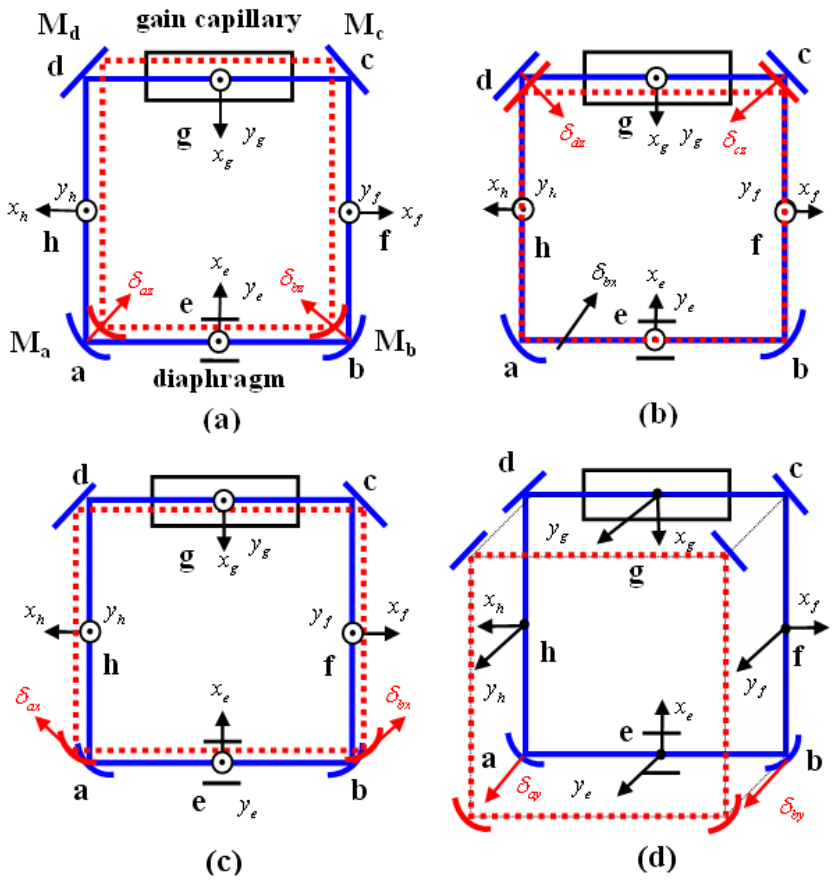

Fig. 4. Schematic diagram of experimental results on optical-axis perturbations in square ring resonator. (a) optical-axis perturbation caused by spherical mirror's axial displacements $\delta_{iz}(i=a,b)$, (b) optical-axis perturbation caused by planar mirror's axial displacements $\delta_{iz}(i=c,d)$, (c) optical-axis perturbation caused by spherical mirror's radial displacements $\delta_{ix}(i=a,b)$ and (d) optical-axis perturbations caused by spherical mirror's axial displacements $\delta_{iy}(i=a,b)$. The ideal optical-axes and the real optical axes after special perturbations are represented by blue solid lines and red dashed lines respectively, spherical mirror's positions after axial displacements and radial displacements are illustrated with red solid arcs, and planar mirror's positions after axial displacements are illustrated with red solid lines.

The experimental results are shown with diagrammatic representation in Fig. 4. Optical-axis perturbations caused by spherical mirror's axial displacements $\delta_{iz}(i=a,b)$ and planar mirror's axial displacements $\delta_{iz}(i=c,d)$ are illustrated in Fig. 4(a) and Fig. 4(b) respectively. It can be easily found that $\delta_{iz}(i=a,b,c,d)$ have no contributions to perturbations in sagittal plane such as Δy_e and Δy_g. In addition, the following novel results can be obtained, that spherical mirror's axial displacements δ_{az} and δ_{bz} have contributions on Δx_e and Δx_g, while at the same time, planar mirror's axial displacements δ_{cz} and δ_{dz} have no contributions to Δx_e. Optical-axis perturbation in tangential plane and sagittal plane

#141768 - $15.00 USD Received 26 Jan 2011; revised 13 Mar 2011; accepted 15 Mar 2011; published 24 Mar 2011

which are caused by radial displacements $\delta_{ix}(i=a,b)$ and $\delta_{iy}(i=a,b)$ respectively are illustrated in Fig. 4(c) and Fig. 4(d) accordingly.

4. Analysis of monolithic triaxial ring resonators

Based on the above discussion, we can consider the optical-axis perturbation of MTRR which has been proposed in ref [15]. For a MTRR, all its three planar ring resonators are SRRs which are mutually orthogonal. As shown in Fig. 5, mirrors M_1, M_2, M_3, M_4, M_5 and M_6 are respectively positioned in the center of each cube body face. The cube is machined such that a small diameter bore connects adjacent mirrors. A closed optical cavity is defined between four coplanar mirrors, which are interconnected by bores. There are three mutually orthogonal closed beam paths, each of which is used to detect angular rotation about its normal axis. The planar ring resonator which is defined by the optical cavity between the mirrors M_2, M_3, M_4 and M_6 is called cavity I, the resonator defined by M_1, M_3, M_5 and M_6 is called cavity II, and the resonator defined by M_1, M_2, M_5 and M_4 is called cavity III.

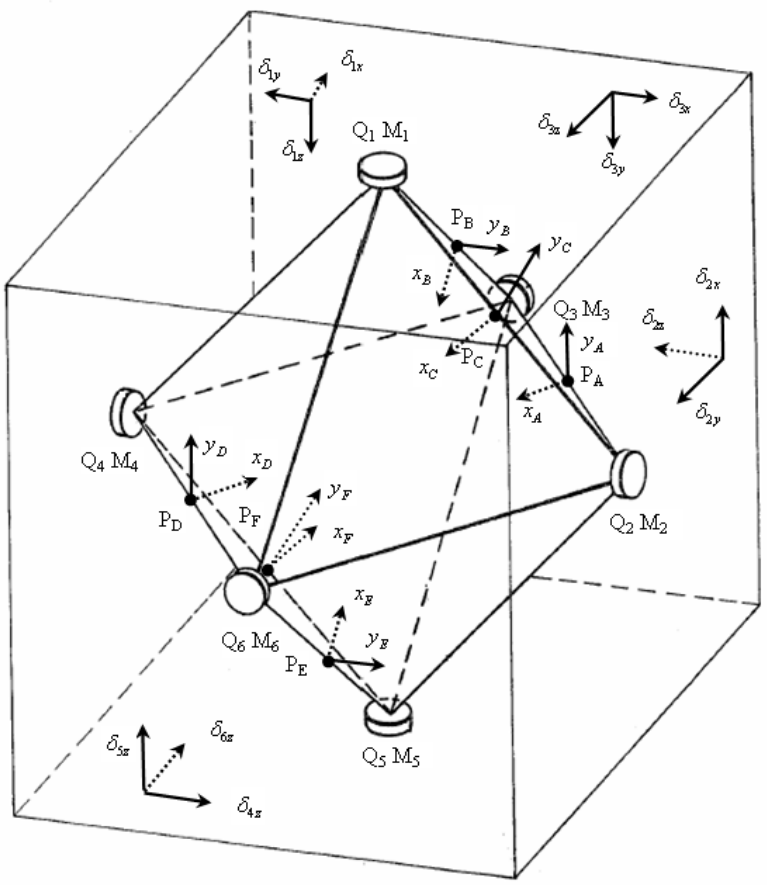

Fig. 5. Schematic diagram of MTRR with all 3 spherical mirror's radial displacements and all 6 mirror's axial displacements. M_1, M_2 and M_3: spherical mirrors with radius R, M_4, M_5 and M_6: planar mirrors, Q_1, Q_2, Q_3, Q_4, Q_5 and Q_6: terminal points of the resonator, P_A:, P_B:, P_C, P_D, P_E and P_B: the midpoints of straight lines Q_2Q_3, Q_1Q_3, Q_1Q_2, Q_4Q_6, Q_5Q_6 and Q_4Q_5 respectively, $\delta_{1x},\delta_{1y},\delta_{2x},\delta_{2y},\delta_{3x},\delta_{3y}$: radial displacements of spherical mirrors M_1, M_2 and M_3, $\delta_{1z},\delta_{2z},\delta_{3z},\delta_{4z},\delta_{5z},\delta_{6z}$: axial displacements of mirrors M_1, M_2, M_3, M_4, M_5 and M_6.

#141768 - $15.00 USD Received 26 Jan 2011; revised 13 Mar 2011; accepted 15 Mar 2011; published 24 Mar 2011

The mirror's angular misalignment-induced optical-axis perturbations in SRR and MTRR have been discussed, and the diaphragm mismatching error C of MTRR has also been found out in previous papers [8, 15, 16]. C cannot be decreased by modifying the angles of the terminal surfaces and the terminal mirrors. In other words, the three monoaxial ring resonators cannot be aligned to pass through the center of their diaphragms simultaneously by angular misalignments. In this paper, the perturbation sources of all 6 mirror's axial displacements and all 3 spherical mirror's radial displacements will be considered. The points P_A, P_B and P_C, which are the diaphragms of the cavities I, II and III, and their symmetrical points P_D, P_E and P_F, which are the center of the gain capillary for each cavity, will be chosen for analysis. For MTRR, it would be better that the optical-axes of all the three monoaxial ring resonators pass through the center of their diaphragms (P_A, P_B and P_C) simultaneously, and this mean the diaphragm mismatching error C should be eliminated [15]. At the same time, it would be much better that the optical-axes of all the three monoaxial ring resonators pass through the center of their gain capillaries (P_D, P_E and P_F) simultaneously too, and this mean the gain capillary mismatching error $C2$ which will be defined in following sections should be eliminated too.

As shown in Fig. 5, δ_{1x}, δ_{1y}, δ_{2x}, δ_{2y}, δ_{3x} and δ_{3y} represent the radial displacements of spherical mirror $M_i(i=1,2,3)$ from time of 0 to t respectively. δ_{1z}, δ_{2z}, δ_{3z}, δ_{4z}, δ_{5z} and δ_{6z} represent the axial displacement of mirror $M_i(i=1,2,3,4,5,6)$ from time of 0 to t respectively. The positive orientations of $x_j, y_j (j=A,B,C,D,E,F)$, are similar to the definitions of Fig. 3 and ref [15]. The optical-axis perturbations at the points P_A, P_B, P_C, P_D, P_E and P_F, caused by all the 3 spherical mirror's translations displacements and all the 6 mirror's axial displacements can be written as

$$\begin{aligned}
\Delta x_A &= \frac{\sqrt{2}}{4}[\delta_{2y}-\delta_{3x}+\delta_{2z}+\delta_{3z}], \Delta y_A = \frac{\sqrt{2}}{2}(\delta_{2x}-\delta_{3y}) \\
\Delta x_B &= \frac{\sqrt{2}}{4}[\delta_{3y}-\delta_{1x}+\delta_{1z}+\delta_{3z}], \Delta y_B = \frac{\sqrt{2}}{2}(\delta_{3x}-\delta_{1y}), \\
\Delta x_C &= \frac{\sqrt{2}}{4}[\delta_{1y}-\delta_{2x}+\delta_{1z}+\delta_{2z}], \Delta y_C = \frac{\sqrt{2}}{2}(\delta_{1x}-\delta_{2y})
\end{aligned} \tag{6}$$

and

$$\begin{aligned}
\Delta x_D &= \frac{\sqrt{2}}{4}[\delta_{2y}-\delta_{3x}-\delta_{2z}-\delta_{3z}+2\delta_{4z}+2\delta_{6z}], \Delta y_D = \frac{\sqrt{2}}{2}(\delta_{2x}-\delta_{3y}) \\
\Delta x_E &= \frac{\sqrt{2}}{4}[\delta_{3y}-\delta_{1x}-\delta_{1z}-\delta_{3z}+2\delta_{5z}+2\delta_{6z}], \Delta y_E = \frac{\sqrt{2}}{2}(\delta_{3x}-\delta_{1y}) \\
\Delta x_F &= \frac{\sqrt{2}}{4}[\delta_{1y}-\delta_{2x}-\delta_{1z}-\delta_{2z}+2\delta_{4z}+2\delta_{5z}], \Delta y_F = \frac{\sqrt{2}}{2}(\delta_{1x}-\delta_{2y})
\end{aligned} \tag{7}$$

Following the expression in ref [15, 16], we can obtain the following equations

$$\begin{aligned}
&\Delta x_A + \Delta y_A/2 + \Delta x_B + \Delta y_B/2 + \Delta x_C + \Delta y_C/2 = \frac{\sqrt{2}}{2}(\delta_{1z}+\delta_{2z}+\delta_{3z}) \\
&\Delta x_C + \Delta y_D/2 + \Delta x_E + \Delta y_E/2 + \Delta x_F + \Delta y_F/2 \\
&= \frac{\sqrt{2}}{2}(2\delta_{4z}+2\delta_{5z}+2\delta_{6z}-\delta_{1z}-\delta_{2z}-\delta_{3z})
\end{aligned} \tag{8}$$

That is different from the results of optical-axis perturbation caused by the mirror's angular misalignments where it is 0 in ref [15]. We use the functions of

#141768 - $15.00 USD Received 26 Jan 2011; revised 13 Mar 2011; accepted 15 Mar 2011; published 24 Mar 2011

$x_j(t), y_j(t)(j = A,B,C,D,E,F)$ to represent the optical-axis locations those 6 points at the time of t. $x_j(0), y_j(0)(j = A,B,C,D,E,F)$ is used to represent the optical-axis locations at the time of $t = 0$. The optical-axis perturbations during the period of time from 0 to t can be written as:

$$\begin{aligned} \Delta x_j(0 \to t) &= x_j(t) - x_j(0) \\ \Delta y_j(0 \to t) &= y_j(t) - y_j(0), j = A,B,C,D,E,F \end{aligned} \tag{9}$$

According to Eq. (8),

$$\begin{aligned} &\sum_{j=A,B,C} \Delta x_j(0 \to t) + \Delta y_j(0 \to t)/2 = \frac{\sqrt{2}}{2}(\delta_{1z} + \delta_{2z} + \delta_{3z}) \\ &\sum_{j=D,E,F} \Delta x_j(0 \to t) + \Delta y_j(0 \to t)/2 = \frac{\sqrt{2}}{2}(2\delta_{4z} + 2\delta_{5z} + 2\delta_{6z} - \delta_{1z} - \delta_{2z} - \delta_{3z}) \end{aligned} \tag{10}$$

By using the following definition of mismatching error C and $C2$, and utilizing Eq. (9) and Eq. (10), we can obtain

$$\begin{aligned} C(t) &= \sum_{j=A,B,C} x_j(t) + y_j(t)/2 \\ &= \sum_{j=A,B,C} x_j(0) + y_j(0)/2 + \frac{\sqrt{2}}{2}(\delta_{1z} + \delta_{2z} + \delta_{3z}) = C(0) + \frac{\sqrt{2}}{2}(\delta_{1z} + \delta_{2z} + \delta_{3z}) \end{aligned}$$

$$\begin{aligned} C2(t) &= \sum_{j=D,E,F} x_j(t) + y_j(t)/2 \\ &= \sum_{j=D,E,F} x_j(0) + y_j(0)/2 + \frac{\sqrt{2}}{2}(2\delta_{4z} + 2\delta_{5z} + 2\delta_{6z} - \delta_{1z} - \delta_{2z} - \delta_{3z}) \\ &= C2(0) + \frac{\sqrt{2}}{2}(2\delta_{4z} + 2\delta_{5z} + 2\delta_{6z} - \delta_{1z} - \delta_{2z} - \delta_{3z}) \end{aligned} \tag{11}$$

$C(t)$ is the total spatial displacements between the ideal optical-axes and the real optical-axes of the cavities I, II and III at the locations of their diaphragms. $C2(t)$ is the total spatial displacements between the ideal optical-axes and the real optical-axes of the cavities I, II and III at the locations of their gain capillaries. $C(t)$ is called the diaphragm mismatching error and $C2(t)$ is called the gain capillary mismatching error in this paper. The distances between the optical axis and the center of the diaphragm at any point of P_A, P_B, P_C and their symmetrical point P_D, P_E and P_F at the time of t can be written as $D_A(t)$, $D_B(t)$, $D_C(t)$, $D_D(t)$, $D_E(t)$ and $D_F(t)$ [15],

$$D_j(t) = \sqrt{x_j(t)^2 + y_j(t)^2}\,(j = A,B,C,D,E,F) \tag{12}$$

Obviously, when $C(0) \neq 0$, the three monoaxial ring resonators cannot be aligned to the best condition of $D_A(0) = D_B(0) = D_C(0) = D_D(0) = D_E(0) = D_F(0) = 0$. In order to make the total diffraction loss of the monolithic triaxial ring resonator be lowest, the values of $D_A(0)$, $D_B(0)$, $D_C(0)$, $D_D(0)$, $D_E(0)$ and $D_F(0)$ should be made smallest. That is to say that the diaphragm mismatching error C should be shared equally [15]. So the best case should be

#141768 - $15.00 USD Received 26 Jan 2011; revised 13 Mar 2011; accepted 15 Mar 2011; published 24 Mar 2011

$$
\begin{aligned}
&x_A(0) = x_D(0) = x_B(0) = x_E(0) = x_C(0) = x_F(0) = C/3 \\
&y_A(0) = y_D(0) = y_B(0) = y_E(0) = y_C(0) = y_F(0) = 0 \\
&D_A(0) = D_B(0) = D_C(0) = D_D(0) = D_E(0) = D_F(0) = \frac{|C|}{3}
\end{aligned} \tag{13}
$$

Now let us look back to the Eq. (11), the result in ref [15] is not valid now. The diaphragm mismatching error $C(t)$ and gain capillary mismatching error $C2(t)$ of the MTRR is not invariant and it can be variable because of spherical and planar mirror's axial displacements. Whatever the mismatch errors C and $C2$ of the MTRR at the time of $t = 0$ is big or small, C and $C2$ at the time of t can be decreased and even eliminated to 0 by choosing appropriate δ_{1z}, δ_{2z}, δ_{3z}, δ_{4z}, δ_{5z} and δ_{6z}. If the following conditions have been satisfied:

$$
\begin{aligned}
&\delta_{1z} + \delta_{2z} + \delta_{3z} = \sqrt{2} \times C(0) \\
&\delta_{4z} + \delta_{5z} + \delta_{6z} = \sqrt{2} \times C(0)
\end{aligned} \tag{14}
$$

And the simplest case is

$$
\begin{aligned}
&\delta_{1z} = \delta_{2z} = \delta_{3z} = \sqrt{2} \times C(0)/3 \\
&\delta_{4z} = \delta_{5z} = \delta_{6z} = \sqrt{2} \times C(0)/3,
\end{aligned} \tag{15}
$$

then the following ideal condition can be obtained:

$$
\begin{aligned}
&C(t) = 0, C2(t) = 0 \\
&x_A(t) = x_B(t) = x_C(t) = x_D(t) = x_E(t) = x_F(t) = 0 \\
&y_A(t) = y_B(t) = y_C(t) = y_D(t) = y_E(t) = y_F(t) = 0 \\
&D_A(t) = D_B(t) = D_C(t) = D_D(t) = D_E(t) = D_F(t) = 0
\end{aligned} \tag{16}
$$

$D_A(t)$, $D_B(t)$, $D_C(t)$, the distances between the optical axis and the center of the diaphragm at any point of P_A, P_B, P_C have been made smallest. At the same time, $D_D(t)$, $D_E(t)$ and $D_F(t)$, the distances between the optical axis and the center of the gain capillary at any point of P_D, P_E, P_F have been made smallest too. The total diffraction loss of the monolithic triaxial ring resonator has been made lowest.

Cavities I, II and III of MTRR are SRRs, so the alignment experimental setup for MTRR is similar to the setup for SRR. Three sets of experimental setup as shown in Fig. 3(b) are used to align the three SRRs of MTRR simultaneously.

The alignment processes of MTRR are similar to the alignment process of SRR which has been discussed in previous section. During the first step, the optical-axes of three set of CCD areas and focusing lens have been made aligned with the ideal optical-axes of cavities I, II and III of MTRR respectively. During second step, the optical-axes of three set of incidental lasers have been made aligned with the three ideal optical-axes of the cavities I, II and III respectively too. Third step, the incidental lasers (HNLP) are adjusted and the frequencies of the input lasers are modified, when the input frequencies have resonances with passive ring cavity I, II and III simultaneously. When the perturbation sources of $\delta_{iz}(i = 1,2,3,4,5,6)$ and $\delta_{ix}, \delta_{iy}(i = 1,2,3)$ is added to the mirrors of passive ring cavity, the real optical axes will be modified with respect to the ideal optical-axes of the passive ring cavity accordingly.

As a consequence, the rules of optical-axes perturbations have been obtained and the results in above theoretical analysis have been confirmed. Experimental results on the method for sharing and eliminating the mismatching errors C and C2 in SRR of MTRR is illustrated

#141768 - $15.00 USD Received 26 Jan 2011; revised 13 Mar 2011; accepted 15 Mar 2011; published 24 Mar 2011

in Fig. (6). Cavity I is SRR of MTRR and it has been chosen as example to describe its optical-axis perturbation during the mismatching error sharing process and mismatching errors eliminating process. The ideal optical-axis of cavity I without any perturbation sources is illustrated in Fig. 6(a). Without any elimination method, every single monoaxial ring resonator of the MTRR have to share the diaphragm mismatching error C in the three specific directions of x_A, x_B and x_C equally described as Eq. (13). Optical-axis perturbation of the cavity I during this sharing process has been illustrated in Fig. 6(b).

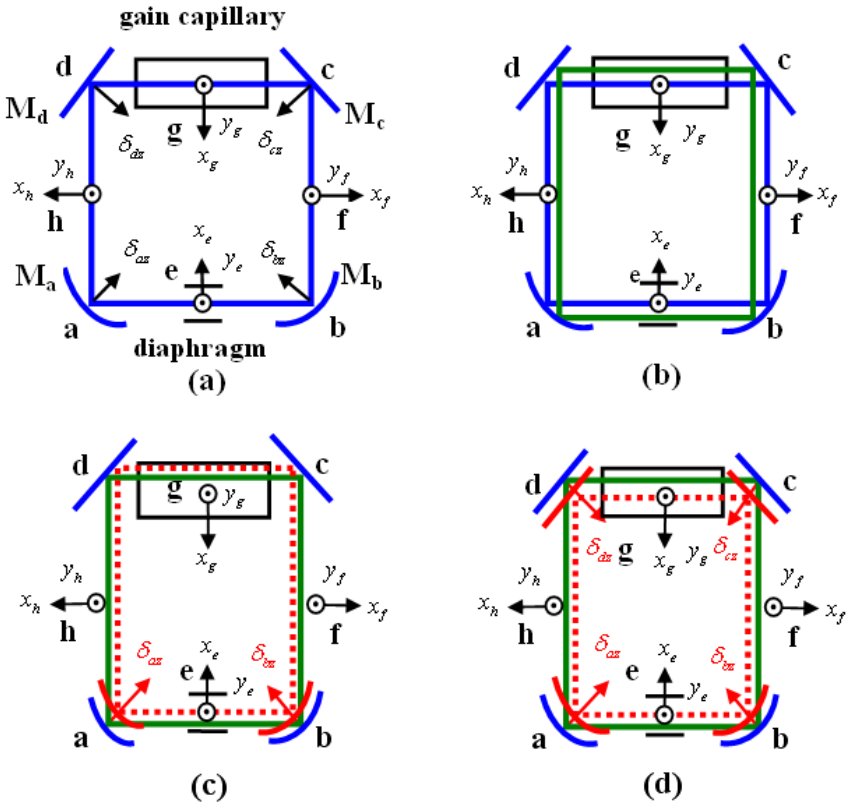

Fig. 6. Schematic diagram of experimental results on the method for sharing and eliminating the mismatching errors C and C2 in SRR of MTRR. (a) ideal optical-axis of SRR, (b) optical-axis perturbation of SRR during mismatching error sharing process, (c) optical-axis perturbation of SRR during the mismatching error eliminating process by utilizing spherical mirror's axial displacements $\delta_{iz}(i=a,b)$, and (d) optical-axis perturbation of SRR during the eliminating process by utilizing both spherical and planar mirror's axial displacements $\delta_{iz}(i=a,b,c,d)$. The ideal optical-axis, the optical-axis after the mismatching error sharing process and the optical axis after the mismatching error eliminating process are represented by blue solid line, green solid line and red dashed line respectively, spherical mirror's positions after axial displacements are illustrated with red solid arc, planar mirror's positions after axial displacements are illustrated with red solid line.

The Optical-axis perturbation of the cavity I during the elimination process by utilizing the previous elimination method is illustrated in Fig. 6(c) [16], and the Optical-axis perturbation of the cavity I during the elimination process by utilizing the novel elimination method is illustrated in Fig. 6(d). As shown in Fig. 6(c), with the eliminating method which has been proposed in ref [16]. and by utilizing spherical mirror's axial displacements $\delta_{iz}(i=a,b)$ as described in Eq. (14, 15), the optical-axes of all the three monoaxial ring resonators of MTRR

#141768 - $15.00 USD Received 26 Jan 2011; revised 13 Mar 2011; accepted 15 Mar 2011; published 24 Mar 2011

can be made to pass through the center of their diaphragms, but meanwhile they deviate from the center of their gain capillaries. As shown in Fig. 6(d), by utilizing both spherical and planar mirror's axial displacements $\delta_{iz}(i=a,b,c,d)$ as described in Eq. (14, 15), the optical-axes of all the three monoaxial ring resonators of MTRR can be made to pass through the center of their diaphragms and the center of their gain capillaries simultaneously.

It is worthwhile to note that the mirrors axial displacement cannot be modified during alignment process, even if the path length control device is added to the mirrors after the alignment process, the mirror's modifying range is still limited. So, in our experiment, the diaphragm mismatching error $C(0)$ and gain capillary mismatching error $C2(0)$ of MTRR will be measured first in the first alignment process, then the ring cavity block will be sent back to be machined. The eliminating process will been accomplished by controlling the allowances of the terminal faces of the ring cavity block and $\delta_{iz}(i=1,2,3,4,5,6)$ are modified as described in Eq. (14, 15). At last, the diaphragm mismatching error $C(t)$ and gain capillary mismatching error $C2(t)$ of MTRR will be reduced to 0 in the second alignment process.

5. Conclusion

In summary, to the best of our knowledge, for the first time in this paper, the generalized ray matrix has been proposed, which is an augmented 5×5 ray matrix for spherical mirror reflection with all the possible perturbation sources including two kinds of angular misalignments and three kinds of translational displacements. A detailed coordinate system for deducing the ray matrix has also been proposed here. SRR and MTRR have been chosen as examples to show its application. Based on the augmented 5×5 ray matrix method by considering all four mirror's axial displacements and two spherical mirror's radial displacements in SRR, some novel results of the optical-axis perturbation have been obtained. By applying those results in three SRRs of a MTRR, the diaphragm mismatching error C of the MTRR has been found out that it does not has any relation with the planar mirror's axial displacement and it has the relation with the spherical mirror's axial displacement. The gain capillary mismatching error C2 of the MTRR has been defined in this paper. A novel method to eliminate the diaphragm mismatching error C and the gain capillary mismatching error $C2$ more effectively and simultaneously by controlling the spherical and planar mirror's axial displacements has been proposed. By utilizing this method, the diaphragm mismatching error C and gain capillary mismatching error $C2$ can be reduced to 0. That is to say, the optical-axes of all the three monoaxial ring resonators of MTRR can be made to pass through the center of their diaphragms and the center of their gain capillaries simultaneously. All these novel results in SRR, MTRR and the eliminating method for MTRR have been confirmed by our alignment experiment. The results have been described in detail with diagrammatic representation. This generalized ray matrix is valuable for ray analysis of various kinds of resonators. These results are important for the cavity design, cavity improvement and alignment of high accuracy and super high accuracy SRR and MTRR laser gyroscopes.

Acknowledgments

This work was supported by the National Science Foundation of China under grant 61078017 and 60608002.

#141768 - $15.00 USD Received 26 Jan 2011; revised 13 Mar 2011; accepted 15 Mar 2011; published 24 Mar 2011